

Chapter 1: Account for Random Microstructure in Multiscale Models

Vadim V. Silberschmidt

Wolfson School of Mechanical and Manufacturing Engineering,
Loughborough University, Ashby Road, Loughborough, Leics.,
LE11 3TU, UK

1.1 Introduction

The accumulated in last decades knowledge of fibre-reinforced composite materials, their effective properties as well as deformation and damage processes in them confirms a random (probabilistic) character of their failure (see, e.g. [1–4] and references therein). Such a character is determined by the specificity of microstructure of composites – a result of a manufacturing process of embedding of a huge number of reinforcing elements into a matrix. The resulting microscopic heterogeneity linked to randomness in positions of fibres, their bonding with the matrix, presence of microdefects, etc. causes a spatially and temporally non-uniform response to external loading even under macroscopically uniform loading conditions. The resulting pattern of deformation localisation and stress concentrations is neither uniform nor periodic; it defines macroscopic non-uniformity in evolution of various damage mechanisms.

At the current level of computational facilities, direct introduction of these stochastic microscopic features into computational models is prohibitive and counterproductive. A significantly better strategy is to employ multiscale models [5] that separate the levels of descriptions into (at least) local and global ones. The local level is used to incorporate details of a (real) microstructure of composites within a relatively small area (window) and to study the effect of its variability while the global one accounts for geometry of composite components/structures and loading/environmental conditions to study problems of their macroscopic behaviour, structural

integrity and/or durability. But such separation of scales presupposes a necessity to bridge them within a framework of a single computational approach. Generally, various schemes to account for material's randomness can be employed both for various scales of modelling and bridging procedures.

The diversity of composites (in terms of constituents, their morphology and a type of reinforcement) makes a general analysis of their behaviour, including damage accumulation, practically infeasible. Hence this chapter is limited to analysis of the effect of randomness in distributions of filaments in matrix on damage evolution in two-phase fibrous composites under external load. A vast literature on composites that assumes a periodic character of reinforcement is not considered here (though some of its results are employed as an obvious comparison basis). Since only plies of unidirectional (continuous) fibre-reinforced composites are considered, the orientational randomness of inclusions is also not treated here. Though 3D studies and simulations are becoming a routine approach, and the respective experimental techniques, e.g. micro-X-ray computer tomography, can provide necessary volumetric data, for the sake of more 'transparency' a local modelling level in this chapter is limited to (predominantly) 2D analysis of unidirectional layers in the plane perpendicular to its fibres. This is due to the emphasis on transverse (matrix) cracking in cross-ply laminates, which is one of their main damage mechanisms under static and fatigue loading conditions [2, 4]. So, effectively, the (virginal) state of transverse cross-section of plies in such composites can be considered as a 2D distribution of circular inclusions in a matrix (Fig. 1.1).

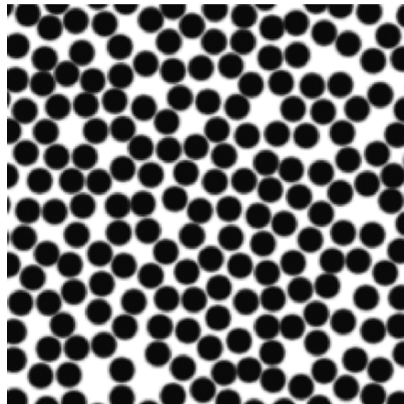


Fig. 1.1. Distribution of continuous graphite fibres in epoxy matrix in a transverse cross-section of a unidirectionally reinforced ply (digitalisation of a micrograph)

This chapter treats various aspects of randomness at various levels of modelling of fibre-reinforced cross-ply laminates – from the character of local distributions of fibres to non-uniformity of damage processes and cracking evolution and their influence on the composite’s response to external loading.

1.2 Microstructures and Effective Properties

Though microstructural randomness of composites was obvious to researchers from the very beginning of the studies of such materials, the main emphasis of research was on the determination of their overall properties that could allow the use of deterministic continuous descriptions. In other words, an inhomogeneous material (discrete medium) is substituted by an equivalent homogenous one (continuous medium). This can be implemented by means of homogenisation procedures, ‘smearing’ microscopic features at the macroscopic level of modelling. In many cases, an assumption of a *coherent mixture* or *statistical homogeneity* is employed: The spatial distribution of the phases is assumed to be macroscopically homogeneous [6–11]. But even in this case, a full description of a composite with arbitrary geometry of phases and their volume fractions is cumbersome, so the emphasis is shifted to estimates of the effects of structural and microscopic features (volume fractions, shape of filaments, the extent of randomness in their distributions, variations in dimensions, etc.). The implementation of all of the mentioned factors within the framework of a single model is a rather complicated task, so historically effects of a single feature (or of a few ones) were studied separately. The research started for cases with so-called ‘dilute dispersions’ [6], i.e. low-volume fractions of reinforcement in a matrix, to exclude the effects due to their interactions, but later on it was extended to arbitrary volume fractions.

The main line of analysis was a use of periodic arrays of reinforcement in a matrix. Though micrographs of real microstructures vividly demonstrated deviations from regular patterns in distributions of inclusions (Fig. 1.1), (relative) simplicity of the approach made it very attractive. The notion of *representative volume*, used to estimate the effective properties, is also introduced early in the study of composites. According to Hill [6], it means a sample with two main properties:

1. Its structure is ‘entirely typical’ for the composite.
2. It contains a ‘sufficient number’ of microstructural elements so that boundary conditions at the surface of the composite do not affect its effective properties.

The main schemes used to determine the effective properties of composites are either the direct approaches, using, e.g. Voigt and Reuss estimates based on assumptions of uniform distributions of the stress and strain, respectively, or variational ones, employing, for instance, an elastic polarisation tensor [12]. The latter scheme allows one to obtain much closer bounds for the effective moduli than the Voigt and Reuss estimates. The well-known *Hashin–Shtrikman bounds* are determined on the basis of the original variational approach; the classical extremum principles of mechanics are used in [13] to obtain bounds for the overall elastic properties of an inhomogeneous system composed of various solid phases at arbitrary concentrations with ideal bonding.

The obtained results and bounds for elastic moduli explicitly depend on the volume fraction of constituents, or, for a two-phase composite, on the volume fraction of reinforcement due to an apparent relation

$$V_f + V_m = 1, \quad (1.1)$$

where V_f and V_m are volume fractions of reinforcement (fibres) and matrix, respectively.

For a case of fibre-reinforced composites with continuous fibres, one of the first results for bounds of the effective elastic moduli for a case of a transversely isotropic composite with fibres of the same diameter, arranged in a hexagonal array, was obtained in [9]. More general results for a case of arbitrary geometry, restricted to the statistically transversal isotropy, are obtained in [14]. At the same time, Hashin [14] noted that it was ‘not known how to use statistical details of phase geometry in prediction of macroscopic elastic behaviour’. The solution was based on the analysis performed for a cylindrical sub-region, extending from base to base of the fibre-reinforced specimen (Hashin introduced there the well-known now abbreviation RVE for *representative volume element*) with its transverse cross-section being, on the one hand, considerably smaller than that of the entire specimen but, on the other hand, considerably larger than that of the filament.

The Hashin’s approach deals with a ‘cylinder assemblage’ by contrast with the ‘concentric composite circular cylinders’ of Hill [7]. Both approaches provide the same bounds for the transverse plain-strain bulk modulus for a two-phase fibre-reinforced composite. Still, these approaches predicted a relatively broad interval of effective properties important for various application magnitudes of the volume fraction of fibres $V_f \approx 0.55$.

To improve the obtained bounds, approaches based on multi-point correlation functions were introduced. An example of such a function is the n -point probability function [15, 16]

$$S_n(\mathbf{x}_1, \mathbf{x}_2, \dots, \mathbf{x}_n) = \left\langle \prod_{i=1}^n I(\mathbf{x}_i) \right\rangle, \quad (1.2)$$

where $I(\mathbf{x})$ is the *characteristic function* (known also as *indicator function* [17]) of the phase 1 (e.g. inclusions)

$$I(\mathbf{x}) = \begin{cases} 1, & \text{if } \mathbf{x} \text{ belongs to phase 1,} \\ 0, & \text{otherwise;} \end{cases} \quad (1.3)$$

angular brackets denote an ensemble average.

The volume fraction V_f is a one-point probability function. The two-point probability function $S_2^{(i)}(\mathbf{x}_1, \mathbf{x}_2)$ for a phase i of a composite can be interpreted as a probability that two points at positions \mathbf{x}_1 and \mathbf{x}_2 belong to this phase [18]. For statistically isotropic media, the two-point probability function depends only on the distance $r = |\mathbf{x}_1 - \mathbf{x}_2|$ between the points, and the simplified notation $S_2^{(i)}(r)$ can be used. For a statistically isotropic fibrous composite, two estimates hold

$$S_2^f(0) = V_f \quad (1.4)$$

and

$$\lim_{r \rightarrow \infty} S_2^f(r) = V_f^2. \quad (1.5)$$

Such correlation functions are normally referred to as *microstructural descriptors*, a thorough review of various types of which is given in [17].

To introduce the extent of connectedness of microstructural elements into consideration (that the two-point probability function lacks), another statistical measure – *lineal-path function* – is introduced in [19]. This parameter denoted $L_2^{(i)}(\mathbf{x}_1, \mathbf{x}_2)$ is linked to the probability that a line segment spanning from \mathbf{x}_1 and \mathbf{x}_2 is situated entirely in the phase i .

Three-point correlation functions are employed in [20] to obtain the bounds for elastic properties of composites. One disadvantage of the approach is the use of different correlation functions to define the upper and lower bounds of properties. So, Milton [21, 22] introduced ‘simplified bounds’ for two-component composites that depend on the volume fraction of two ‘fundamental geometric parameters’ $\xi_1 = 1 - \xi_2$ and $\eta_1 = 1 - \eta_2$ ($\xi_i, \eta_i \in [0,1]$). These bounds are more restrictive than the Hashin–Shtrikman bounds (up to five times narrower according to Milton [21]); the latter correspond to cases $\xi_1 = \eta_1 = 0$ and $\xi_1 = \eta_1 = 1$. The self-consistent

approximations of [11, 23] correspond – to the same order of approximation – to $\xi_1 = \eta_1 = V_f$. The fourth-order correlation functions for composites are suggested in [24].

An alternative approach to the self-consistent scheme is introduced in [25, 26] and coined *differential effective medium theory* in [26]. According to Norris [27], the suggested approach is rooted in the idea of Roscoe [28] that extended the famous Einstein’s results on suspensions [29, 30]. One of the advantages of the differential scheme – as compared to the self-consistent one – is that it distinguishes between the two phases. One phase is taken as a matrix while the second – filament – is incrementally added to it from zero concentration to the final value [25, 27]. At each stage of the process, the added inclusions are considered to be embedded in a homogeneous material, corresponding to the composite formed by the matrix and all the previously added inclusions. This process is described by the tensorial differential equation of the following structure:

$$\frac{d\mathbf{L}}{dV_f} = \frac{1}{1-V_f}(\mathbf{L}_1 - \mathbf{L})\mathbf{E}_1, \quad (1.6)$$

with an obvious condition

$$\mathbf{L}(V_f = 0) = \mathbf{L}_2. \quad (1.7)$$

Here \mathbf{L} is the (fourth-order) tensor of effective moduli of the two-phase composite; \mathbf{L}_1 and \mathbf{L}_2 are moduli of inclusions and matrix, respectively; $\mathbf{E}_1 = [\mathbf{I} + \mathbf{P}(\mathbf{L}_1 - \mathbf{L})]$ is a strain concentration tensor; \mathbf{I} is a unit tensor and tensor \mathbf{P} was introduced by Hill [23]. A more generalised scheme is suggested in [27], where ‘particles’ of both matrix and inclusions can be added simultaneously to the initial material.

1.3 Microstructures and Their Descriptors

Since transversal arrangements of fibres in unidirectional layers of real composites are vividly random (Fig. 1.1), researchers trying to adequately describe them are confronted with several problems:

1. Characterisation of random microstructures
2. Comparison of random and periodic microstructures
3. Introduction of real microstructures into models

The first problem is traditionally solved with the help of the automatic image analysis (AIA) and various tessellation schemes. An attempt to

quantify the random distribution of filaments (second phase) in a matrix by means of AIA and Dirichlet cell tessellation procedures was undertaken in [31, 32]. Voronoi tessellation, based on discretisation of a domain into multi-sided convex polygons (known as *Voronoi*) each containing no more than a single filament, is also used to estimate the character of distribution of distances between filaments [33, 34]. The distribution of cells is supposed to be of the Poisson type with the cumulative probability distribution function accounting for non-overlapping assemblage of filaments (known as *Gibbs hard-core process*)

$$P(\hat{V}_f > V_f) = 1 - \exp \left[-\frac{\bar{V}_f}{1 - \bar{V}_f} \left(\frac{1}{V_f} - 1 \right) \right]. \tag{1.8}$$

It describes the cumulative probability that the local volume fraction of fibres \hat{V}_f exceeds a value V_f ; \bar{V}_f denotes a mean volume fraction. In the case of the unidirectional 2D composite with random fibre spacing $V_f = h/c$, where h and c are a fibre radius and a half-spacing between (centres of) neighbouring fibres, respectively (Fig. 1.2). The corresponding probability density function has the following form [34]:

$$p(V_f) = \frac{\bar{V}_f}{1 - \bar{V}_f} \frac{1}{V_f^2} \exp \left[-\frac{\bar{V}_f}{1 - \bar{V}_f} \left(\frac{1}{V_f} - 1 \right) \right]. \tag{1.9}$$

The *exact* relation for the probability density function for inter-fibre spacing x in the case of random impenetrable fibres of unit diameter is obtained in [35, 36]

$$p(x) = \frac{\bar{V}_f}{1 - \bar{V}_f} \exp \left[-\frac{\bar{V}_f}{1 - \bar{V}_f} (x - 1) \right]. \tag{1.10}$$

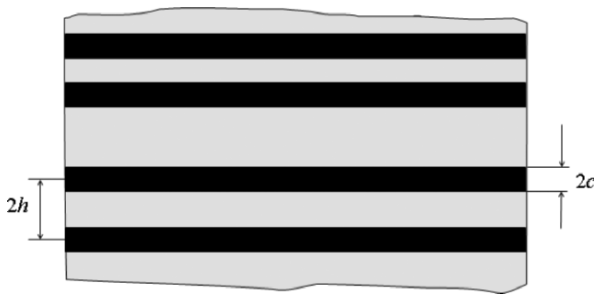


Fig. 1.2. Longitudinal cross-section of unidirectional fibre-reinforced composite

A study of micrographs of a carbon fibre-reinforced PEEK prepreg, containing about 2,000 fibres with the volume fraction close to 50%, has shown that the distribution of Voronoi distances – distances in an arbitrary direction from the centroid of a fibre to the Voronoi cell boundary – can be assumed as a random one [37]. The Voronoi distance is also used as a random variable of the statistical description suggested in [38].

1.3.1 Parameters of Microstructure

Various parameters are introduced to quantify the extent of non-uniformity in distributions of filaments in composites. Several such parameters are suggested in [39]. The first one – *homogeneity distribution parameter* ξ – characterises the closeness of N particles (e.g. fibres in a transversal cross-section) within the window with area A

$$\xi = \frac{d_p}{\sqrt{A/N}}. \quad (1.11)$$

This parameter is a ratio of two magnitudes of an inter-particle distance, one, d_p , corresponding to the peak of probability density diagram for this parameter and another being an effective average of it. Obviously, for a square lattice $\xi = 1$; its value diminishes with the increase in clusterisation. Another parameter – an *anisotropy parameter of the first kind* η – can also be applied to a distribution of cylindrical fibres in a transversal cross-section. It is introduced as [39]

$$\eta = \frac{1}{N} \sum_{i=1}^N \cos 2\theta_i, \quad (1.12)$$

where θ_i is an orientation angle for the direction from the centre of the window to the centroid of particle i . For a statistically isotropic distribution, this parameter should vanish.

Several parameters are suggested to characterise the extent of clustering and the properties of clusters (see, e.g. [40]). Still, in traditional carbon fibre-reinforced composites with $V_f \geq 0.5$, the clusters are less obvious (if at all) than in metal matrix composites (MMCs).

As it is shown in [41], real distributions of fibres in unidirectional composites are neither periodic nor fully random, thus presupposing employment of measures that provide additional quantitative characteristics of the exact type of microstructures. So, based on the works of Ripley [42, 43], a *second-order intensity function* $K(r)$ was introduced to describe distributions of points in the following form [41]:

$$K(r) = \frac{A}{N^2} \sum_{k=1}^N \frac{I_k(r)}{w_k}. \quad (1.13)$$

This function characterises the expected number of further points (e.g. centres of fibres) within the distance r from an arbitrary point, normalised by their intensity (i.e. the number of points per unit area). Here, A is an area of the sampling window, containing N points, and $I_k(r)$ is the number of points situated within the distance r from the point k . The weighting factor w_k is introduced to account for the edge effects; it is equal to the ratio of the circumference of the circle situated within the window. If the entire circle with radius r is situated within the window, $w_k = 1$ and it is smaller than unity otherwise. The second-order function was applied to specimens of unidirectional fibre-reinforced composites exposed to different levels of external pressure during curing; also statistics for orientations and distances between fibres were used in terms of cumulative distribution functions. It was shown that these parameters, obtained with the use of image analysis from micrographs of real specimens, significantly differ from those of artificial microstructures with the same number of fibres, obtained by the Poisson process [41]. Unfortunately, second-order functions are not able to determine sub-patterns in distributions, so either parameters of a higher order or combinations of second-order functions with some other parameters should be used [44].

The second-order intensity function $K(r)$ can also be used to derive another quantitative parameter, characterising randomness in distribution of fibres (their centroids). It can be introduced in the following way [41, 44, 45]. The average number of fibre centroids located within a circular ring of radius r and thickness dr with a centre at a given fibre centroid is

$$dK(r) = K(r + dr) - K(r). \quad (1.14)$$

Dividing (1.14) by the area of the ring $2\pi r dr$, one can obtain the local spatial density of fibres. The ratio of the latter and the average spatial density N/A forms the *radial distribution function* [41, 45]

$$g(r) = \frac{A}{2\pi r N} \frac{dK(r)}{dr}. \quad (1.15)$$

Obviously, for a random Poisson process $g(r) = 1$. The value r_0 , for which $g(r_0) = 1$, is a characteristic scale of the local disorder in an ensemble.

In parallel with statistical characterisation of distributions of microscopic features (e.g. filaments in a matrix) in composites, various topological characteristics are introduced. An obvious development in this direction is application of fractals [39, 46, 47].

A multifractal formalism can provide useful information on the type of the random distribution of fibres in the matrix [48]. It characterises the spatial scaling of non-uniform distributions: A local probability (number of fibres) P_i in the i th box (element) from a set of boxes, compactly covering the area of interest, scales with the box size l as

$$P_i(l) \propto l^{\alpha_i}, \quad (1.16)$$

where the scaling exponent α_i is known as *singularity strength*. According to the multifractal theory [49, 50], the number of elements with probability characterised by the same singularity strength is linked to the box size by the fractal (Hausdorff) dimension $f(\alpha)$

$$N(\alpha) \propto l^{-f(\alpha)}. \quad (1.17)$$

The function $f(\alpha)$, known as *multifractal spectrum*, describes the continuous (but finite) spectrum of scaling exponents for a random distribution. As it was shown in [48], the distribution of carbon fibres in epoxy matrix is multifractal; the respective multifractal spectrum was calculated.

1.3.2 Local Volume Fraction

Analysing the effects of microstructural randomness, an obvious idea is to consider the volume fraction of reinforcement not only in terms of a global description, i.e. as a parameter characterising the entire composite, but also as a field function, introducing the idea of a *local volume fraction*. A direct comparison of various parts of the composite (Fig. 1.3) vividly demonstrates that the volume fraction of fibres depends on a location in a composite. In Torquato [17], it is introduced as an average over a volume element (observation window) V_0 of the composite with the centroid at \mathbf{x}

$$V_f(\mathbf{x}) = \frac{1}{V_0} \int_{V_0} I(\mathbf{x}) \theta(\mathbf{x} - \mathbf{z}) d\mathbf{z}, \quad (1.18)$$

where $I(\mathbf{x})$ is the characteristic function (see (1.3)), \mathbf{z} characterises any point in V_0 and $\theta(\mathbf{x} - \mathbf{z})$ is the indicator function

$$\theta(\mathbf{x} - \mathbf{z}) = \begin{cases} 1, & \mathbf{z} - \mathbf{x} \in V_0, \\ 0, & \text{otherwise.} \end{cases} \quad (1.19)$$

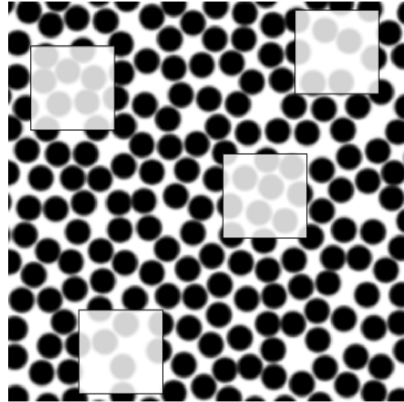


Fig. 1.3. Variations in local volume fraction of fibres (see Fig. 1.1)

Obviously, the size of V_0 will affect the level of the local volume fraction; but even for the same V_0 it depends on \mathbf{x} . All the moments of this variable are studied for various systems in [51].

Two schemes are used in [52] to estimate variability of the volume fraction in carbon–epoxy T300/914 unidirectional composite. For macroscopic specimens with a cross-section 10×1 mm, a direct measurement of the Young’s modulus of the composite is employed to calculate V_f using a linear rule of mixtures. An image analysis of fields 0.1×0.1 mm provides the data for direct estimation of the volume fraction of fibres (and its variation). In both cases, the distributions peak at (or close to) the nominal volume fraction $V_f = 0.6$. The increase in the window dimension results in the decrease in the scatter; still, even for a macroscopic specimens of the first method the measured interval of V_f was from 0.5 to 0.68.

Another analysis is performed for a micrograph of the ply’s cross-sectional area of a carbon/epoxy composite, containing 603 fibres with diameter $d^f = 10 \mu\text{m}$ [48]; the size of the window is $345 \times 250 \mu\text{m}$ (its part is shown in Fig. 1.1). With the increase in the window size, the distribution of local magnitudes of V_f changes its shape and bounds – maximal (V_f^{\max}) and minimal (V_f^{\min}). The respective evolution of these bounds is shown in Fig. 1.4. For sufficiently small window size, these two bounds demonstrate mono-phase asymptotes: $V_f^{\max} \rightarrow 1$ and $V_f^{\min} \rightarrow 0$. With the increase in the window size, both bounds should converge to the average value

$$V_f^{\max} \rightarrow \bar{V}_f \quad \text{and} \quad V_f^{\min} \rightarrow \bar{V}_f. \quad (1.20)$$

Though this trend is distinct in Fig. 1.4, the full convergence of the bounds is not reached even at the length scale of 115 μm .

The spatial variation in the volume fraction of fibres causes considerable variations in the local values of stiffness: For the window size 30 μm , the axial and shear moduli demonstrate the scatter of more than 100% and the transverse module more than 40%.

An important parameter of local variations of the volume fraction of fibres V_f , treated as a random variable, can be linked to the standard deviation of its local magnitude. Such a parameter, named *coarseness* C , is introduced in [15, 36] as the standard deviation of the volume fraction of filaments normalised by its mean value \bar{V}_f

$$C = \frac{1}{\bar{V}_f} \sqrt{\langle V_f^2 \rangle - \bar{V}_f^2}. \quad (1.21)$$

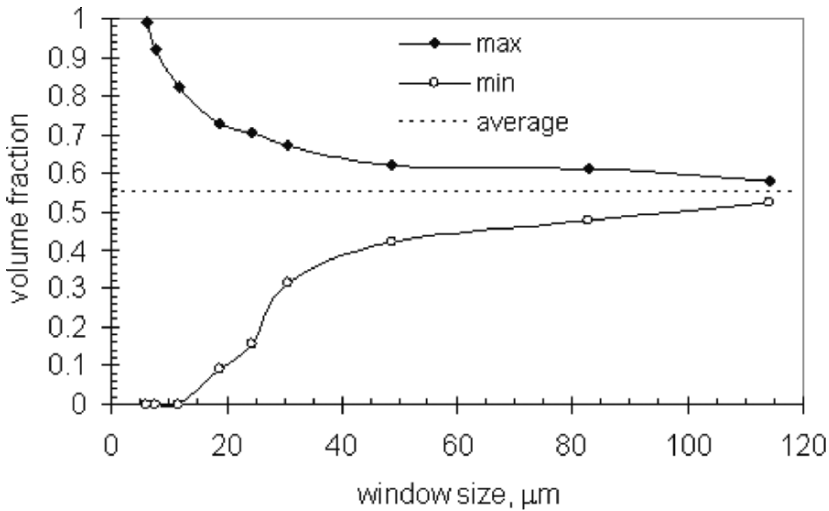


Fig. 1.4. Evolution of bounds for local volume fraction with window size

The change of coarseness C with the window size, calculated for the arrangement of 603 fibres that was treated before (see Fig. 1.4), is presented in Fig. 1.5. Obviously, $C = 0$ for an infinite area.

1.4 RVE Size

The problem of transferability of results obtained for some part of the composite's cross-section cannot be solved without the knowledge of representativeness of these results. This, in its turn, necessitates determination of the RVE size (or sizes). Obviously, a problem of the minimum size of the RVE for a random media – one of the central questions in the study of such materials – is linked to the analysed property/process and is not a universal parameter, depending purely on morphology of reinforcement. It is defined by the type of the property, the property's contrast in a composite and the volume fraction; the chosen precision of approximation plays a very important part in this as well as the type of the boundary conditions [53].

A diversity of ways to characterise and quantify microstructures and their randomness leads to various schemes for definition of the minimum RVE size. For instance, the last parameter from Sect. 1.3.2 – coarseness C – can be used for this purpose, linking the minimum RVE size to implementation of the condition of closeness of C to zero. Some notions of RVE (see one by Hill above) either explicitly or implicitly introduce ways to determine the respective minimum size. Still, in many cases this process leads to very large dimensions of RVEs, so that they could contain a sufficient number of microstructural elements to ensure the statistical representativeness.

The radial distribution function $g(r)$ (see Fig. 1.15) was also suggested as a basis to define the minimal RVE size. The latter is considered to be the value of radius r_0 , for which $g(r_0) = 1$.

Another notion, employed in [54], is introduced with regard to the overall modulus $\widehat{\mathbf{L}}$ that will provide a sufficiently correct link between average (macroscopic) stresses and strains

$$\langle \boldsymbol{\sigma} \rangle = \widehat{\mathbf{L}} \langle \boldsymbol{\varepsilon} \rangle, \quad (1.22)$$

where angular brackets denote averaging. Normalising contribution of the non-local terms for simple cases of materials (non-overlapping spheres in a matrix) and deformation (varying normal strain and shear strain), it is possible to obtain explicit estimates. In the cases with extreme contrasts – rigid inclusions or voids – the RVE size practically does not exceed two reinforcement diameters for 5% error of $\widehat{\mathbf{L}}$ [54]. Even for a case of higher precision (error 1%), this size for the most demanding cases of matrix–reinforcement combinations is less than 5 diameters. This is confirmed by numerical studies of overall properties of non-linear composites with random distributions of fibres [55].

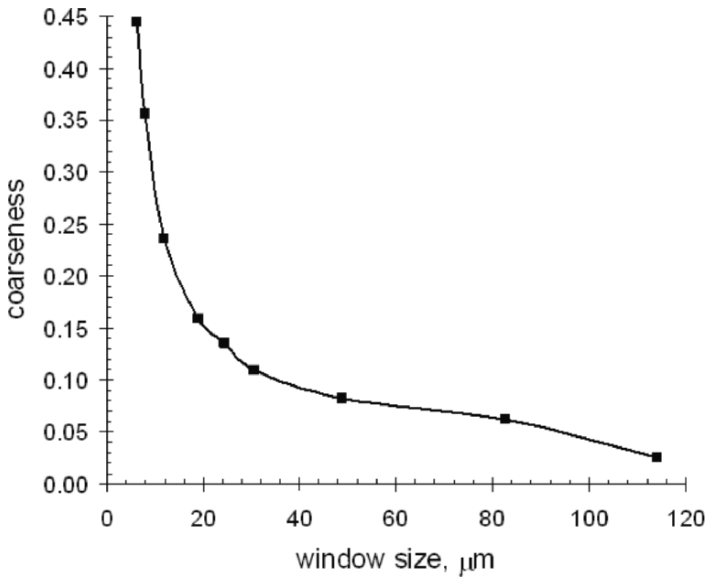


Fig. 1.5. Evolution of coarseness with window size

1.5 Periodic vs. Random

Determination of the RVE size allows considering two inter-linked problems: comparison of periodic arrangements of reinforcements with random ones and introduction of random microstructures into modelling schemes. The latter can be implemented by a direct incorporation of microstructural morphology from obtained micrographs into various computational schemes (e.g. by means of discretisation of digitalised images into finite elements) with a subsequent numerical solution of the problem. But since transferability of this ad hoc solution to other areas even of the same composite is, at least, questionable, special procedures of the microstructure's *reconstruction* were developed; they will be treated in Sect. 1.6.

Generally, a vivid deviation of real microstructures from periodic ones initiated their comparison at the early stages of the history of micro-mechanics of composites [56]. Obvious advantages of the use of periodic arrangements of fibres in studies and simulations – from existence of analytical estimates to possibility of high-refined meshes for very small windows – impelled researchers to compare those arrangements with real (random) microstructures to study reducibility of the latter to the former.

Since the manufacturing of periodic arrangements for large number of microscopic reinforcing elements is cumbersome, the main tool for such comparisons is computational analysis. Hence, in studies of composite materials, a considerable emphasis has been on a comparison of random and non-random models and their closeness to experimental results for composites.

The data obtained by combination of the image analysis and Dirichlet cell tessellation procedures [31, 32] are used to numerically generate distributions of reinforcements with the same average magnitudes and standard deviations. Numerical simulations, performed for various periodic and random distributions of fibres with different shapes of their cross-sections for boron fibre-reinforced aluminium, have vividly demonstrated a significant influence of microstructural features on the composite's effective elastic moduli as well as on the plastic flow/localisation. The case with a random distribution of circular fibres (30 fibres were used in a statistical realisation) in a transverse cross-section provided the closest match to experimentally measured values [57]. It is worth mentioning that the effect of fibres' distributions on the material's response is relatively stronger than that of their shape.

For a unidirectional fibre-reinforced boron–aluminium composite ($V_f = 0.48$), models for square and hexagonal arrays and a random distribution were compared with experimental data for components of stiffness and compliance [58]. Two experimental methods were used to estimate those components: the ultrasonic-velocity method and the resonance method. It is demonstrated that the random distribution model provides the best approximations to the measured parameters.

An extensive study of the periodic and random distributions of fibres in matrix and their effect on transverse properties is implemented in [55] with the employment of Fast Fourier Transforms as an alternative to finite element analysis. A window of $1,024 \times 1,024$ pixels is used to resolve an area of non-linear composite (with elasto-plastic matrix) containing 64 fibres ($V_f = 0.475$) with a resolution 128×128 pixels per fibre. The main result for effective properties is that the scatter in the transversal Young's moduli is small (standard deviation is less than 1%) while the flow stress and hardening modulus demonstrate higher fluctuations. Another approach is used in [44] based on the perturbed periodic square arrays of fibres with clustered or staggered patterns that are compared with a square one. These less ordered patterns are generated by a shift of the centre of a circular cross-section of a fibre in a unit cell (each containing a single fibre) from its fully symmetrical position in a square array. Combined with a special type of boundary conditions, this scheme allows simulations of unidirectional continuously reinforced MMCs with the volume fraction of

fibres, similar to the previous example. The obtained results for a boron–aluminium MMC demonstrate that the axial overall response is practically independent of the arrangement of fibres, while the transverse parameters (both the elastic moduli and yield limits) are highly sensitive to it.

Another study [59], based on the boundary element method, compared square and hexagonal arrangement of fibres with random ones, using the *embedded cell approach*. The latter is implemented by embedding the core, containing a discrete arrangement of fibres (60 fibres in random cores), into a homogeneous media with properties obtained, e.g. by the self-consistent scheme, to which the far-field boundary conditions are applied. It was shown that the fibre packing arrangement significantly affects the overall stress distribution as well as the extent of stress localisation, with considerably higher stress concentrations observed in random sets. For instance, for carbon fibre/epoxy composite ($V_f = 0.56$) 90% higher local radial stresses are reported in [60] for a random arrangement as compared to a hexagonal one. This can be naturally explained by the fact that some morphological parameters of random microstructures differ from those of periodic ones. An obvious example is the nearest-neighbour distances for random and clustered distributions are smaller than those for square or hexagonal patterns [61].

A detailed analysis of the effect of arrangement of fibres on stress concentration was undertaken in [62]. The studied microstructures included 600 fibres in a matrix with the contrast in the Young's modulus 6.7 and close Poisson's ratios. The volume concentration of reinforcement was 0.1 and the minimum distance between the centroids of reinforcements was three times their radius. The main conclusion is that the proximity of reinforcements along the direction of loading results in the highest stress concentration. Alignments of fibres, close to each other, along directions at large angles to the loading one cause the stress reduction.

To account for the effect of the relative positions of, and orientations between, neighbouring fibres, a special *stress interaction parameter* was introduced in [63]. This is an additional descriptor used to quantify a short-range configuration of fibres

$$c = \min_i \min_j \left[d_{ij} \left(1 + \frac{\theta_{ij}}{\alpha} \right) \right]. \quad (1.23)$$

Here d_{ij} is a distance between centroids of two fibres i and j ; θ_{ij} is the angle between the line connecting them and the loading direction; $\alpha = \pi/3$ is a normalising factor. The lower c , the higher the radial stress concentration.

An attempt is also made to determine parameters of a periodic microstructure, similar to a random two-phase microstructure [64]. It employs discretisation of the image of the actual microstructure and calculation of its power spectral density. Then parameters of the unit cell are chosen: number of reinforcements, their geometry, initial dimensions of the cell and positions of reinforcements. Since the discrete power spectral densities of the original and equivalent systems are obtained under various conditions (e.g. frequencies), the so-called ‘rebinning’ [64] process is used to match the frequencies. The final positions of particles in the unit cell are found with the use of the minimisation of a specially constructed function.

1.6 Direct Introduction of Microstructure

Understanding of (sometimes) considerable deviations of microstructures of real composites from periodic ones resulted in an obvious idea of a direct introduction of such a microstructure into numerical schemes. Two principal ways to implement this are possible (1) direct use of a scanned microstructural images and (2) generation of artificial microstructures. While the former procedure is relatively straightforward, the latter one raises the question of reproducibility of main features of the material. A somewhat simplified way for a 2D case of a transversal cross-section is to introduce a ‘fully random’ system using, e.g. a planar Poisson process for hard-core (i.e. impenetrable) disks [65]. An obvious deficiency of this approach is that it is not linked to the exact type of stochasticity of the microstructure that can deviate from the ideal randomness. Hence, it is necessary to reflect the features (at least principal ones) of an original microstructure in the artificially generated microstructure of the composite.

Naturally, a direct account for random features of the microstructure began in micromechanical models. One of the typical examples is the introduction of the random fibre spacing [66, 67]. A random number generator is used to produce a set of random numbers that, after re-ordering in an ascending order, present the set of transversal co-ordinates z_m for parallel fibres in a 2D set. The fibre spacing d_m is then defined in an obvious way

$$d_m = z_{m+1} - z_m \quad (1.24)$$

with the average spacing being

$$d_0 = \frac{1}{N-1} \sum_1^{N-1} d_m = \frac{1}{N-1} (z_{m+1} - z_m), \quad (1.25)$$

where N is the total number of fibres.

Several statistical realisations for sets of 12 fibres are used in calculations of the stress concentration factors (SCFs); both the average and the variance of the distribution of spacing are equal to unity. To exclude an overlap of neighbouring fibres, a lower cut-off at some arbitrary chosen level is introduced. A transition from the deterministic case with a uniform distribution of fibres in a transversal direction results in a statistical character of magnitudes of SCFs in the composite.

A more consistent approach to reflect the original microstructure and its features in a model was named *reconstruction* (e.g. [18]) and is understood as generation of the microstructure employing the correlation functions, characterising its morphology.

The suggested variant of this procedure for a two-phase statistically isotropic material is based on two-point correlation functions, introduced for two digitized representations of the microstructure – original, with the reference correlation function $f_0(r)$, and ‘reconstructed’ (i.e. generated), with $f_s(r)$. Manipulation of the generated image, using interchanges of the states for pairs of arbitrarily selected pixels of two phases to preserve the volume fraction, is controlled by minimisation of a variable E that plays the role of energy in this approach [18]

$$E = \sum_i [f_s(r_i) - f_0(r_i)], \quad (1.26)$$

where r is the distance between two points. The probability of acceptance of such phase interchange, estimated after each step, is determined by the energy change for two subsequent steps ΔE

$$p(\Delta E) = \begin{cases} 1, & \Delta E < 0, \\ \exp(-\Delta E / T), & \Delta E > 0. \end{cases} \quad (1.27)$$

Here T plays the role of temperature.

The suggested scheme converges to the reference correlation function $f_0(r)$. It is worth mentioning that the general framework can be used with a variety of correlation functions. The authors used two functions – the two-point probability function and lineal-path function – since they characterise various facets of real microstructures, e.g. the former is good in catching the short-range information while the latter contains information on connectedness. One of the suggested ways to expand this description is to account for various correlation functions in the expression for energy,

modifying it to accommodate various functions with some weights [18]. Reconstructions of random microstructures, based on two mentioned functions, though demonstrated a rather good match for the reference and artificial microstructure, still resulted in some deviations from the original, as measurements with other correlation functions have shown. Another way for reconstruction of the microstructure is suggested in [68], based on the maximum entropy principle.

An alternative variant to generate of a periodic unit cell, based on the data on statistic features of the composite's microstructure, is suggested in [69]. For a fibre-reinforced composite material characterised by a given second-order intensity function $\bar{K}(r)$ (see (1.13)), which is evaluated in points r_i , $i = 1, \bar{N}_m$, positions of centroids of N fibres in a 2D unit cell with dimensions $H_1 \times H_2$ are defined by means of the following relation

$$\mathbf{x}_{H_1, H_2}^N = \arg \min_{\mathbf{x} \in \mathbf{S}} F(\mathbf{x}_{H_1, H_2}^N), \quad (1.28)$$

where

$$F(\mathbf{x}_{H_1, H_2}^N) = \sum_{i=1}^{N_m} \left(\frac{\bar{K}(r_i) - K(r_i)}{\pi r_i^2} \right)^2.$$

Here, vector $\mathbf{x} = \{x_i, y_i\}$, $i = \overline{1, N}$, defines positions of the centroids in the unit cell and \mathbf{S} denotes a set of admissible \mathbf{x} . A numerical realisation can be implemented with the use of genetic algorithms [69].

A so-called *mean-window technique* [70], based on the exact averaging over the volume fraction, can also be used as a basis to generate model microstructures with statistical functions, similar to observed/measured ones. It allows estimating effective properties of a composite by averaging randomly selected windows from a real structure, as obtained from a micro-tomographic analysis. The suggested method exploits the hypothesis of ergodicity, according to which an ensemble average of a property obtained on smaller volumes is equal to the average over an infinite one [71]. Authors also distinguish between the physical and geometrical RVEs. The latter has a standard sense as a material volume of specific size (e.g. equal to the correlation length of the two-point probability function [71]). In contrast, the *physical RVE* (PRVE) is defined by the level of variation of the physical property, which should become insignificant for a PRVE. One of the possible formulations for the PRVE is that of a minimum material volume for which the standard deviation for different statistical realisations is smaller than the measurement error for a chosen parameter. Applicability

of the mean-window technique is restricted to fulfilment of two conditions [71] (1) symmetry of the probability distribution function and (2) linearity of the variation of the chosen property within the respective interval of the local volume fraction, for a given window size. Another feature affecting the size of this PRVE is the contrast of properties (i.e. the ratio of elastic moduli of the matrix and reinforcement): An increase in the contrast will request a larger window.

1.7 From Micro to Macro: A Way to Multiple Scales

The choice of the adequate dimensions for the RVE and introduction of the (principal) microstructural features, though complying with requirements of representativeness, still do not always allow a direct transfer of the results, obtained for some area (window) to a real component/structure. There are several reasons for this:

1. The results, obtained for an RVE, will depend on the type of the employed boundary conditions: homogeneous strain or stress, periodic, etc. [53, 72].
2. A transfer of loads/environmental conditions, externally applied to a macroscopic component, to the RVE can be implemented in various ways.
3. Gradients in stress and/or strain fields due to non-uniform loading or stress concentration as well as edge effects affect the results.

Still, RVE with periodic boundary conditions is broadly used to estimate the effective properties of heterogeneous materials with a given type of microstructure. More advanced schemes have been introduced to overcome the discussed limitations and to develop more adequate modelling tools. One possibility is to use a *meso-scale window* as an alternative to the RVE [73, 74]. The window is placed within a two-phase domain and its size L (and the respective non-dimensional window scale $\delta = L/d$, where d is the size of inclusions) is being changed to determine a convergence condition for two responses of an elastic heterogeneous media, controlled by either stresses or strains. Calculations, based on two respective types of boundary conditions, preclude the necessity to use periodic boundary conditions within the RVE formalism, still providing bounds for stiffness for any δ . Random simulations (using Monte Carlo sampling) employ approximations of the planar continuum by a very fine spring network, with respective stiffness magnitudes depending on coordinates. A detailed analysis

of probability density distributions shows that the beta distribution can properly describe variations in the local stiffness without truncations; if truncations are acceptable then Chi, Gumbel max, Rayleigh and Gauss distributions can be used for this purpose [74]. Generally, RVE is considered as a deterministic limit of a statistical volume element (SVE) in [75].

An alternative to the RVE formalism is an approach based on lattice models that was initially developed for problems of statistical physics [76]. In application to materials with spatial randomness in their properties, linked to their microstructure, it employs not a single RVE but a set of them – each with its own properties – compactly covering the area of interest [48, 77–79].

Another approach is the scheme named *Voronoi cell finite element method* [80, 81] that is an extension of the Dirichlet tessellation. Each of the Voronoi polygons of such tessellation, containing a single filament, is treated as a finite element. This representation of microstructure, which can be linked to image analysis data, is used as a basis for a two-level computational model for heterogeneous materials [81]. A two-way linkage between the levels is introduced in the following way:

1. Data from the microscopic level are used to estimate the global effective parameters of the composite at each point of the macroscopic level.
2. Macroscopically calculated data are used to determine the distribution of stresses and strains in the microstructure.

This scheme goes back to the first attempts to introduce multiscale modelling schemes (though the term was suggested considerably later) for composites. Their necessity has always been obvious: numerical simulations based on the finite elements method (or any comparable schemes), accounting for the exact position of all the fibres in the whole specimen is not practical since dimensions of the elements should be considerably smaller than the diameter of a fibre. With the latter being, e.g. 5–10 μm for carbon fibres, the simulation of a standard composite specimen becomes prohibitive at the current level of computational power. Hence, to overcome this obstacle, the problem was separated into solvable sub-tasks. One of the typical approaches is to limit a microscopic analysis with a sufficient resolution of microstructural elements to a relatively small area of interest of the component, with the component itself being analysed within the framework of a macroscopic mechanics, i.e. employing of the effective properties. In Akbarzadeh and Adams [82], the following two-step procedure is used:

1. A macroscopic analysis of the whole region (homogeneous and transversely isotropic in the case of [82])
2. A micromechanical analysis of the region of interest containing several fibres with the boundary conditions obtained from the previous stage

The results for a notch area of the Charpy specimen for a random distribution of fibres (in total, four fibres are situated in the studied microscopic area) have demonstrated that the microscopic features can have a profound effect on the global behaviour: It can be more important for stress localisation than the curvature of the notch [82].

Still, the random character of materials and of deformational and failure processes in them should not be always limited to the microscopic level of their description.

1.8 Randomness at Macroscale

Microstructural (local) randomness of heterogeneous materials does affect their response at the global (macroscopic) level. Here two principal trends are vivid. On the one hand, the increase in the considered area (volume) ‘smoothens’ local fluctuations of properties linked with the microstructure – similar to an averaging procedure for larger sets – thus resulting in the decreasing variability of the global effective properties for macrovolumes (or *twin specimens*). On the other hand, mechanisms causing spatial localisation of deformation and/or fracture processes, for instance, plastic flow and crack nucleation and/or propagation, inherit some of the randomness of the underlying microscopic structure.

Even in the latter case, there is no direct mapping of the microstructural stochasticity onto the macroscopic patterns of behaviour. This effect is more pronounced at the stage of the onset of localisation, but weakens with its development due to a strong interaction with additional mechanisms. Fluctuations in the spatial distribution of constituents result in a non-uniform distribution of microscopic stresses. This factor, together with – also non-uniform – distributions of defects, results in considerable variations in plastic flow and/or damage accumulation and transition to formation of macroscopic defects. This scenario is additionally complicated by multiplicity of damage mechanisms and their interactions.

The material’s behaviour at the initial *pre-critical stage* of deformation is characterised by a bulk response of the entire specimen, demonstrating relatively low spatial fluctuations of stresses and/or strains that are roughly proportional to fluctuations in material’s properties caused by its microstructure. With the onset of the *critical* and *post-critical stages*, characterised

by the localisation of deformation and failure processes, the extent of macroscopic non-uniformity can significantly increase. This localisation can also, in its turn, affect the global material's behaviour. For instance, in composites with elastic–ideal plastic matrix in many cases, only a small part of the matrix participates in the plastic flow, the spatial pattern of which directly affects the overall flow stress of the composite, as shown in [55].

Thus, the macroscopic randomness can be considered as a given feature of a composite only at some stages of its life; in many cases it changes as due to its interaction with loading/environmental conditions. One of the striking examples is evolution of matrix cracking in cross-ply laminates under axial tensile loading. This process starts relatively early in the loading history of composites: at low external stretching under quasi-static loading or during initial cycles of tensile fatigue. Distributions of transverse cracks along the longitudinal axis of cross-ply composites are random: Twin specimens demonstrate various numbers and positions of matrix cracks [83–86]. A typical character of evolution of matrix cracking in a single specimen during its loading history is given in Fig. 1.6. Even in the same specimens, with matrix cracks not crossing their entire width, the crack distribution along two longitudinal edges is different – and random [87].

1.8.1 Evolution of Matrix Cracking

The evolution of matrix cracking, reflected in a pattern of transverse cracks, is a result of interplay of processes of cracks' nucleation and their interaction. At the initial stage of loading history, the macroscopically applied external load accelerates damage evolution in places of stress concentrations and/or largest or preferably oriented microdefects (microcracks, voids, fibre debonding, etc.). This development causes a practically uncork-related generation of matrix cracks with inter-crack spacing demonstrating a high extent of randomness (Fig. 1.6a,b).

Generation of matrix cracks, crossing the entire thickness of a weak 90° layer, causes a significant change in the pattern of stress distributions, especially in this layer. Instead of the longitudinally uniform – if temporarily to neglect variations due to the microstructural randomness for the simplicity of our analysis – field of the axial stress, a new stress pattern arises: Unloaded zones appear in the direct vicinity of the transverse cracks. They are due to the so-called *shielding effect* caused by the traction-free surfaces of the matrix cracks.

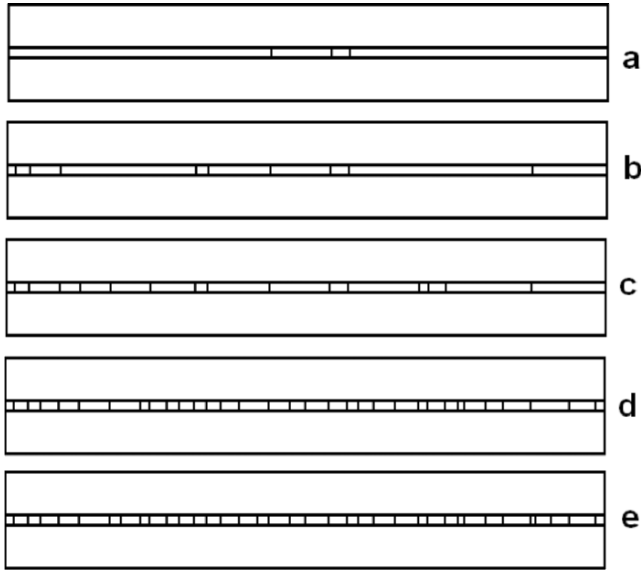


Fig. 1.6. Matrix cracking in a 20 mm long part of $[0_7/90]_s$ carbon-epoxy T300/914 specimen at various moments of loading history: (a) 10 cycles; (b) 100 cycles; (c) 1,000 cycles; (d) 10,000 cycles; (e) 100,000 cycles (*different horizontal and vertical scales*)

These unloaded zones have a considerable length in the axial direction – up to several mm. At the initial stages of matrix cracking, characterised by a low crack density, zones from neighbouring cracks practically do not overlap. Still, the areas of the 90° layer, unaffected by matrix cracking (i.e. not partially unloaded), decrease with the increase in the external load or number of cycles. It means that initially spatially uniform conditions with regard to crack nucleation change: Areas situated somewhere in the middle between two neighbouring cracks with a larger spacing become more preferable for matrix cracking. With the further increase in the number of cycles (or the external load/stretching for quasi-static conditions), the number of cracks increases, and the neighbouring unloading zones begin overlapping (interacting). A resulting distribution of the axial stress component, normalised by its far-field magnitude, in a weak layer that was calculated for a part of a real random distribution of matrix cracks with the use of detailed finite element simulations (see [88]) is given in Fig. 1.7.

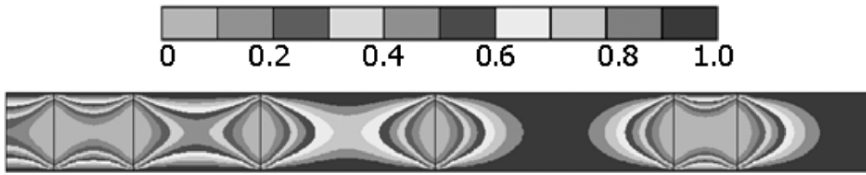


Fig. 1.7. Distribution of the normalised axial stress in a 10 mm long part of 90° layer of $[0_1/90_2]_s$ carbon-epoxy T300/914 composite

Superposition of stress reduction in the areas of overlap causes the additional decline in the probability to initiate a matrix crack in these areas (in some cases the axial stress state can even change from tension to compression). Hence, the stage of random matrix cracking is gradually changed by a more ordered character of transverse crack nucleation, with mid-spacing areas becoming preferable places for this process. Retrieving now the notion of microstructure-induced material's randomness, it is obvious that two major processes determine the pattern of transverse cracks in the 90° layer: The randomness in a spatial distribution of flaws is responsible for spatially non-uniform nucleation of cracks while the re-distribution of macroscopic axial stress orders this process, limiting it to a diminishing part of the composite. Obviously, for the material with a considerable scatter discussed in the previous sections, an event of matrix crack nucleation close to the existing one is still possible if the extent of local stress concentration near a strong flaw is not fully compensated by unloading due to the shielding effect (compare successive stages of the loading history in Fig. 1.6).

The above considerations are based on a one-dimensional interpretation of the process (similar to many modelling schemes that deal with axial stresses, averaged over the thickness of 90° layers). Obviously, the cracking processes in relatively thick layers demonstrate their own specificity as well as in wide specimens; in the latter, under tensile fatigue, matrix cracks do not instantly occupy the entire width of the specimen but grow with random rates [89, 90] (the difference between two schemes also depends on laminate thickness [4]).

Various parameters are used to characterise the randomness of distributions of matrix cracks: the Weibull's distribution [85], number of cracks in bands [2], etc. The multifractal analysis has been found to be a very convenient tool for this purpose [89–91]. It was found that twin specimens, exposed to the same loading history, demonstrate a considerable difference in patterns of transverse cracking (in numbers of cracks and their positions) but their multifractal spectra are very close (see Fig. 1.8).

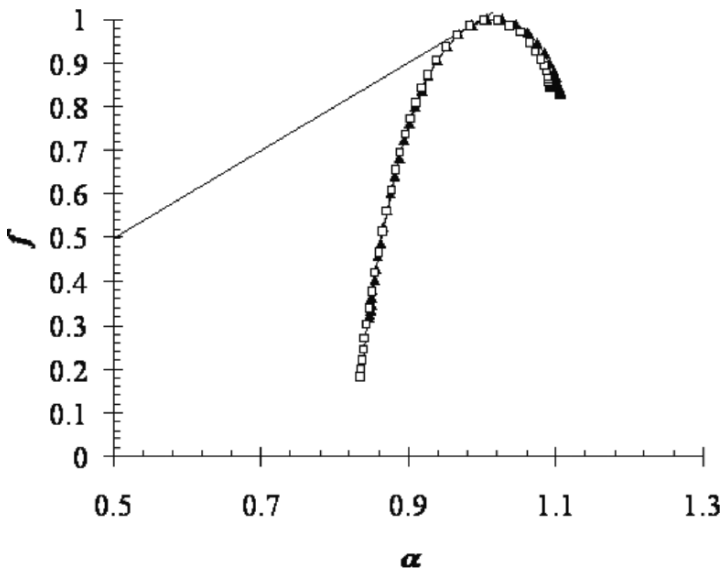


Fig. 1.8. Multifractal spectra of matrix crack sets in two twin specimens of carbon-epoxy T300/914 $[0_2/90_3/0_2]$ laminate loaded with 100,000 cycles ($1,050 \text{ N mm}^{-2}$)

Besides, multifractal spectra depend on both loading conditions and structure of cross-ply laminates (stacking order) (see [92] for a detailed analysis). A typical transformation of $f(\alpha)$ functions with the loading history is given in Fig. 1.9. The width of a multifractal spectrum is linked to an extent of the distribution's randomness: For a fully uniform distribution it is reduced to a single point. Hence, it is possible to interpret the effects of various factors on randomness in matrix cracking.

The initial stage of the tensile fatigue, characterised by a nearly non-restricted (i.e. random) nucleation of matrix cracks, has a rather wide multifractal spectrum (Fig. 1.8). With the increase in the number of cycles, the above described ordering mechanism results in less random patterns of cracks. This is reflected in considerably narrower multifractal spectra. Our results [91, 93] have shown that, for long loading histories when the process of matrix cracking attains the so-called *characteristic damage state* with nearly non-changing distributions of transverse cracks, the respective $f(\alpha)$ functions are very close to each other.

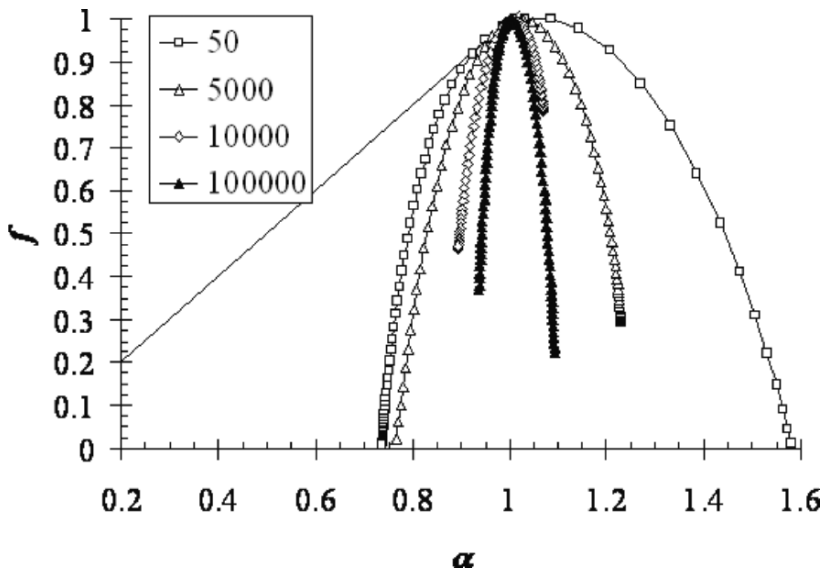


Fig. 1.9. Multifractal spectra of axial distributions of transverse cracks for different number of load cycles

1.8.2 Multi-Mechanism Damage

A detailed analysis of the single damage mechanism in cross-ply laminates allows a better understanding of the macroscopic manifestation of microstructural randomness when one neglects a rather non-trivial interaction between various mechanisms [1]. Here let us consider some of the effects of this mechanism on the macroscopic behaviour of these composites. Firstly, contrary to ideas of the standard approaches, dealing with an area between two neighbouring transverse cracks as a macroscopic RVE, the load (stress) transfer depends also on the exact type of the axial distribution of cracks. It is shown [93] that, at the advanced stages of loading (i.e. in cases of high crack density) for the same spacing, the level of axial stresses both in weak (90°) and stiff (0°) layers differs for different types of crack distributions.

The pattern of matrix cracking affects the distribution of axial cracks and delamination zones in composites. The former are nucleated near $0^\circ/90^\circ$ interfaces close to tips of matrix cracks, while the latter are centred on intersections of transverse and axial cracks [1]. Delamination zones effectively reduce the spacing between neighbouring transverse cracks [92], thus additionally diminishing zones of preferable nucleation for new

cracks (i.e. acting as another ordering mechanism for an ensemble of matrix cracks). Delamination also affects the macroscopic mechanic properties of laminates (e.g. the flexural modulus) to a considerably higher degree than transverse cracking. This effect also depends on the type of the distribution of matrix cracking, showing a considerable scatter in the extent of the modulus' deterioration for the same total length of delamination zones.

Tips of matrix cracks at the $0^\circ/90^\circ$ interfaces cause significant stress concentrations in stiff layers, adjacent to them. Such local overloading can result in fibre breakage and final rapture of the laminate. Here, the randomness in the pattern of stress concentration due to the underlying character of distribution of transverse cracks interacts with other random microstructural features, e.g. non-uniform longitudinal distributions of fibre's strength and fibre debonding areas. Such interaction additionally complicates the scenario of macroscopic damage evolution in composites.

Thus the result of interacting processes linked to microstructural randomness and ordering due to the load re-distributions 'percolates' to other damage mechanisms, affecting its macroscopic response to external loading. This complicated scenario of multi-mechanism damage is hard to adequately reflect in modelling schemes, which in many cases are reduced to either a single-mechanism studies or an explicit analysis of the interaction between mechanisms at the local level.

1.9 Conclusions

The above analysis of only a few features and damage mechanisms in cross-ply laminates – non-uniformity in the distribution of fibres in plies as well as matrix cracking and delamination – vividly demonstrates a challenge facing researchers who are developing modelling schemes for these materials. Though estimation of the effective macroscopic properties of these composites in a virginal state (i.e. without macroscopic defects) is a relatively simple task which can be solved analytically, an adequate description of damage evolution, especially at the stage of nucleation of macroscopic defects, presupposes a totally different strategy. Some elements of analytical schemes (e.g. load transfer rules, etc.) can be effectively used also in this strategy, forming one part of the computational analysis [94, 95].

In general, modelling of damage in composites can be implemented with the use of various multiscale strategies [5]. Not all the suggested multiscale schemes take random features of the microstructure into consideration. Generally, they combine partial solutions (e.g. for specific local

areas, single damage mechanisms or local interactions of a few mechanisms), based on refined descriptions of the microstructure and/or geometry of the induced damage, with global ones that lack the detailedness at the microscopic level but reproduce the exact structure of a composite and macroscopic loading conditions.

A lattice-model approach [48, 78] employs ideas of continuum damage mechanics to link micro and macro levels. This is achieved by introducing a damage parameter as an additional variable at the macroscopic (continuous) level. This parameter characterises evolution of ensemble of microdefects and its macroscopic manifestation. The effect of spatially random microstructure (e.g. due to a stochastic spatial distribution of fibres) is accounted for, in terms of the varying local stiffness, reflecting the experimentally observed scatter. In this case, application of an externally uniform tensile load results in non-uniform distributions of the axial stress and, subsequently, different rates of damage accumulation for different parts of a 90° layer. The attainment of the critical damage concentration (i.e. implementation of the local failure criterion) in any point of this layer results in initiation of a matrix crack. Matrix cracking causes stress re-distribution, including formation of unloaded zones due to the shielding effect. The latter (as some other factors, for instance, a through-thickness stress variation linked to the effects of the stacking order and resin-rich zones) is incorporated by mapping of a (dynamic) matrix of stress coefficients onto the current stress levels in elements.

This approach allows a natural reflection of the interaction of microstructural randomness and additional ordering, imposed by matrix cracking at advanced stages of the loading history. Though this approach has been used for cross-ply laminates under tensile fatigue, it can be expanded to more complicated cases of both structure of laminates and loading conditions. This can be achieved by introducing of additional load transfer mechanisms, as it was implemented in [94].

Inclusion of additional damage mechanisms, necessary to describe multi-mechanism failure in fibre-reinforced cross-ply composites exposed to conditions of high-cycle fatigue, can be achieved by combining physical and continuum modelling tools within another multiscale formalism [96]. It is based on the use of various damage parameters for respective mechanisms – transverse cracking, delamination and fibre breaks – each with its own damage accumulation law, reflecting experimental observations and measurements [96, 97]. In some cases, an additional scale between microscopic and macroscopic ones – a meso-scale – could be introduced to incorporate several damage entities and capture their interaction for a more precise description of respective local perturbations of the stress field [1].

References

1. Talreja R (2006) Damage analysis for structural integrity and durability of composite materials. *Fatigue Fract Eng Mater Struct* 29: 481–506
2. Berthelot JM (2003) Transverse cracking and delamination in cross-ply glass-fiber and carbon-fiber reinforced plastic laminates: static and fatigue loading. *Appl Mech Rev* 56: 1–37
3. Reifsnider KL, Case SW (2002) *Damage tolerance & durability in material systems*. Wiley-Interscience, New York
4. Ladevèze P, Lubineau G, Violeau D (2006) A computational damage micro-model of laminated composites. *Int J Fracture* 137: 139–150
5. Soutis C, Beaumont PWR (eds) (2005) *Multiscale modelling of composite material systems: the art of predictive damage modelling*. Woodhead, Cambridge
6. Hill R (1963) Elastic properties of reinforced solids: some theoretical principles. *J Mech Phys Solids* 11: 357–372
7. Hill R (1964) Theory of mechanical properties of fibre-strengthened materials. I. Elastic behaviour. *J Mech Phys Solids* 12: 199–212
8. Hashin Z (1964) Theory of mechanical behaviour of heterogeneous media. *Appl Mech Rev* 17: 1–9
9. Hashin Z, Rosen BW (1964) The elastic moduli of fiber-reinforced materials. *J Appl Mech* 31: 223–232
10. Hashin Z (1965) Elasticity of random media. *Trans Soc Rheol* 9: 381–406
11. Budiansky B (1965) On the elastic moduli of some heterogeneous materials. *J Mech Phys Solids* 13: 223–227
12. Hashin Z, Shtrikman S (1963) A variational approach to the theory of the elastic behaviour of multiphase materials. *J Mech Phys Solids* 11: 127–140
13. Walpole LJ (1966) On bounds for the overall elastic moduli of inhomogeneous systems I. *J Mech Phys Solids* 14: 151–162
14. Hashin Z (1965) On elastic behaviour of fibre reinforced materials of arbitrary transverse phase geometry. *J Mech Phys Solids* 13: 119–134
15. Lu B, Torquato S (1990) Local volume fraction fluctuations in heterogeneous media. *J Chem Phys* 93: 3452–3459
16. Gibiansky LV, Torquato S (1995) Geometrical-parameter bounds on the effective moduli of composites. *J Mech Phys Solids* 43: 1587–1613
17. Torquato S (2001) *Random heterogeneous materials. Microstructure and macroscopic properties*. Springer, Berlin Heidelberg New York
18. Yeong CLY, Torquato S (1998) Reconstructing random media. *Phys Rev E* 57: 495–506
19. Lu B, Torquato S (1992) Lineal-path function for random heterogeneous materials. *Phys Rev A* 45: 922–929
20. Beran M, Molyneux J (1966) Use of classical variational principles to determine bounds for the effective bulk modulus in heterogeneous media. *Q Appl Math* 24: 107–118
21. Milton GW (1981) Bounds on the electromagnetic, elastic, and other properties of two-component composites. *Phys Rev Lett* 46: 542–545

22. Milton GW (1982) Bounds on the elastic and transport properties of two-component composites. *J Mech Phys Solids* 30: 177–191
23. Hill R (1965) A self-consistent mechanics of composite materials. *J Mech Phys Solids* 13: 213–222
24. Milton GW, Phan-Thien N (1982) New bounds on the effective moduli of two-component materials. *Proc R Soc A* 380: 305–331
25. Boucher S (1974) On the effective moduli of isotropic two-phase elastic composites. *J Compos Mater* 8: 82–89
26. Mclaughlin R (1977) A study of the differential scheme for composite materials. *Int J Eng Sci* 15: 237–244
27. Norris AN (1985) A differential scheme for the effective moduli of composites. *Mech Mater* 4: 1–16
28. Roscoe R (1952) The viscosity of suspensions of rigid spheres. *Br J Appl Phys* 3: 267–269
29. Einstein A (1906) Eine neue Bestimmung der Moleküldimensionen. *Ann Phys* 19: 289–306
30. Einstein A (1911) Berichtigung zu meiner Arbeit “Eine neue Bestimmung der Moleküldimensionen”. *Ann Phys* 34: 591–592
31. Spitzig WA, Kelly JF, Richmond O (1985) Quantitative characterization of second-phase populations. *Metallography* 18: 235–261
32. Brockenbrough JR, Hunt WH Jr, Richmond O (1992) Reinforced material model using actual microstructural geometry. *Scripta Metall Mater* 27: 385–390
33. Davy PJ, Guild FJ (1988) Distribution of interparticle distance and its application in finite-element modeling of composite materials. *Proc R Soc A* 418: 95–112
34. Chung I, Weitsman Y (1994) A mechanics model for the compressive response of fiber reinforced composites. *Int J Solids Struct* 31: 2519–2536
35. Torquato S (1998) Morphology and effective properties of disordered heterogeneous media. *Int J Solids Struct* 35: 2385–2406
36. Torquato S, Lu B (1993) Chord-length distribution function for two-phase random media. *Phys Rev E* 47: 2950–2953
37. Green D, Guild FJ (1991) Quantitative microstructural analysis of a continuous fibre composite. *Composites* 22: 239–242
38. Davy PJ, Guild FJ (1988) The distribution of interparticle distance and its application in finite-element modelling of composite materials. *Proc R Soc A* 418: 95–112
39. Taya M, Muramatsu K, Lloyd DJ, Watanabe R (1991) Determination of distribution patterns of fillers in composites by micromorphological parameters. *JSME Int J: Ser I* 34: 198–206
40. Yotte S, Breyse D, Riss J, Ghosh S (2001) Cluster characterisation in a metal matrix composite. *Mater Charact* 46: 211–219
41. Pyrz R (1994) Quantitative description of the microstructure of composites. Part I. Morphology of unidirectional composite systems. *Compos Sci Technol* 50: 197–208
42. Ripley BD (1976) The second-order analysis of stationary point processes. *J Appl Probab* 13: 255–266

43. Ripley BD (1977) Modelling spatial patterns (with discussion). *J R Stat Soc B* 39: 172–212
44. Pyrz R (2004) Microstructural description of composites, Statistical methods. In: Böhm HJ (ed) *Mechanics of microstructured materials*. Springer, Berlin Heidelberg New York, pp 173–233
45. Bulsara VN, Talreja R, Qu J (1999) Damage initiation under transverse loading of unidirectional composites with arbitrarily distributed fibers. *Compos Sci Technol* 59: 673–682
46. Cross SS (1994) The application of fractal geometric analysis to microscopic images. *Micron* 25: 101–113
47. Summerscales J, Guild FJ, Pearce NRL, Russell PM (2001) Voronoi cells, fractal dimensions and fibre composites. *J Microsc* 201: 153–162
48. Silberschmidt VV (2005) Multiscale modelling of cracking in cross-ply laminates. In: Soutis C, Beaumont PWR (eds) *Multiscale modelling of composite material systems: the art of predictive damage modelling*. Woodhead Publishing, Cambridge, pp 196–216
49. Chhabra AB, Meneveau C, Jensen RV, Sreenivasan KR (1989) Direct determination of the $f(\alpha)$ singularity spectrum and its application to fully developed turbulence. *Phys Rev A* 40: 5284–5293
50. Harte D (2001) *Multifractals: theory and applications*. Chapman & Hall/CRC, Boca Raton
51. Quintanilla J, Torquato S (1997) Local volume fraction fluctuations in random media. *J Chem Phys* 106: 2741–2751
52. Baxevanakis C, Jeulin D, Renard J (1995) Fracture statistics of a unidirectional composite. *Int J Fracture* 73: 149–181
53. Kanit T, Forest S, Galliet I, Mounoury V, Jeulin D (2003) Determination of the size of the representative volume element for random composites: statistical and numerical approach. *Int J Solids Struct* 40: 3647–3679
54. Drugan WJ, Willis JR (1996) A micromechanics-based nonlocal constitutive equation and estimates of representative volume element size for elastic composites. *J Mech Phys Solids* 44: 497–524
55. Moulinec H, Suquet P (1998) A numerical method for computing the overall response of nonlinear composites with complex microstructure. *Comput Meth Appl Mech Eng* 157: 69–94
56. Adams DF, Tsai SW (1969) The influence of random filament packing on the transverse stiffness of unidirectional composites. *J Compos Mater* 3: 368–381
57. Brockenbrough JR, Suresh S, Wienecke HA (1991) Deformation of metal-matrix composites with continuous fibers: geometrical effects of fiber distribution and shape. *Acta Metall Mater* 39: 735–752
58. Datta SK, Ledbetter HM (1983) Elastic constants of fiber-reinforced boron-aluminum: observation and theory. *Int J Solids Struct* 19: 885–894
59. Knight MG, Wrobel LC, Henshall JL (2003) Micromechanical response of fibre-reinforced materials using the boundary element technique. *Compos Struct* 62: 341–352

60. Matsuda T, Ohno N, Tanaka H, Shimizu T (2003) Effects of fiber distribution on elastic–viscoplastic behavior of long fiber-reinforced laminates. *Int J Mech Sci* 45: 1583–1598
61. Everett RK, Chu JH (1993) Modeling of non-uniform composite microstructures. *J Compos Mater* 27: 1128–1144
62. Ganguly P, Poole WJ (2004) Influence of reinforcement arrangement on the local reinforcement stresses in composite materials. *J Mech Phys Solids* 52: 1355–1377
63. Pyrz R, Bochenek B (1998) Topological disorder of microstructure and its relation to the stress field. *Int J Solids Struct* 35: 2413–2427
64. Povirk GL (1995) Incorporation of microstructural information into models of two-phase materials. *Acta Metall Mater* 43: 3199–3206
65. Alzebdeh K, Ostoja-Starzewski M (1996) Micromechanically based stochastic finite elements: length scales and anisotropy. *Probab Eng Mech* 11: 205–214
66. Smith RL (1983) The random variation of stress concentration factors in fibrous composites. *J Mater Sci Lett* 2: 385–387
67. Fukuda H (1985) Stress concentration factors in unidirectional composites with random fiber spacing. *Compos Sci Technol* 22: 153–163
68. Sankaran S, Zabarar N (2006) A maximum entropy approach for property prediction of random microstructures. *Acta Mater* 54: 2265–2276
69. Zeman J, Šejnoha M (2001) Numerical evaluation of effective elastic properties of graphite fiber tow impregnated by polymer matrix. *J Mech Phys Solids* 49: 69–90
70. Xi Y (1996) Analysis of internal structures of composite materials by second-order property of mosaic patterns. *Mater Charact* 36: 11–25
71. Borbély A, Kenesei P, Biermann H (2006) Estimation of the effective properties of particle-reinforced metal–matrix composites from microtomographic reconstructions. *Acta Mater* 54: 2735–2744
72. Ostoja-Starzewski M, Wang X (1999) Stochastic finite elements as a bridge between random material microstructure and global response. *Comput Meth Appl Mech Eng* 168: 35–49
73. Ostoja-Starzewski M (1993) Micromechanics as a basis of random elastic continuum approximations. *Probab Eng Mech* 8: 107–114
74. Ostoja-Starzewski M (1998) Random field models of heterogeneous materials. *Int J Solids Struct* 35: 2429–2455
75. Ostoja-Starzewski M (2002) Microstructural randomness versus representative volume element in thermomechanics. *J App Mech* 69: 25–35
76. Hermann HJ, Roux S (eds) (1990) *Statistical models for the fracture of disordered media*. North-Holland/Elsevier Science, Amsterdam/New York
77. Silberschmidt VV, Chaboche J-L (1994) The effect of material stochasticity on crack–damage interaction and crack propagation. *Eng Fract Mech* 48: 379–387
78. Silberschmidt VV (1997) Model of matrix cracking in carbon fiber-reinforced cross-ply laminates. *Mech Compos Mater Struct* 4: 23–37

79. Silberschmidt VV (2003) Crack propagation in random materials: computational analysis. *Comput Mater Sci* 26: 159–166
80. Ghosh S, Mukhopadhyay SN (1993) A material based finite element analysis of heterogeneous media involving Dirichlet tessellations. *Comput Meth Appl Mech Eng* 104: 211–247
81. Ghosh S, Lee K, Moorthy S (1995) Multiple scale analysis of heterogeneous elastic structures using homogenization theory and Voronoi cell finite element method. *Int J Solids Struct* 32: 27–62
82. Akbarzadeh A, Adams DF (1976) A hybrid finite element micromechanical analysis of composite materials. *Fibre Sci Technol* 9: 277–295
83. Manders PW, Chou T-W, Jones FR, Rock JW (1983) Statistical analysis of multiple fracture in $0^\circ/90^\circ/0^\circ$ glass fibre/epoxy resin laminates. *J Mater Sci* 18: 2876–2889
84. Boniface L, Smith PA, Ogin SL, Bader MG (1987) Observations on transverse ply crack growth in $(0/90_2)_s$ CFRP laminate under monotonic and cyclic loading. In: Matthews FL, Buskell NCR (eds) *Proceedings of 6th International Conference on Composite Materials (ICCM-6) and 2nd European Conference on Composite Materials (ECCM-2)*, Vol. 3. Elsevier Applied Science, Oxford, pp 156–165
85. Bergmann HW, Block J (1992) Fracture/damage mechanics of composites – static and fatigue properties. Institut für Stukturmechanik DLR, Braunschweig (DLR-Mitteilung 92-03)
86. Berthelot J-M, Le Corre J-F (2000) Statistical analysis of the progression of transverse cracking and delamination in cross-ply laminates. *Compos Sci Technol* 60: 2659–2669
87. Lafarie-Frenot MC, Hénaff-Gardin C (1991) Formation and growth of 90 ply fatigue cracks in carbon/epoxy laminates. *Compos Sci Technol* 40: 307–324
88. Silberschmidt VV (2005) Matrix cracking in cross-ply laminates: effect of randomness. *Compos A: Appl Sci Manuf* 36: 129–135
89. Silberschmidt VV, Hénaff-Gardin C (1996) Multifractality of transverse cracking and cracks' length distribution in a cross-ply laminate under fatigue. In: Petit J (ed) *ECF 11. Mechanisms and mechanics of damage and failure*, Vol. 3. EMAS, London, pp 1609–1614
90. Silberschmidt VV (1998) Multifractal characteristics of matrix cracking in laminates under T-fatigue. *Comput Mater Sci* 13: 154–159
91. Silberschmidt VV (1995) Scaling and multifractal character of matrix cracking in carbon fibre-reinforced cross-ply laminates. *Mech Compos Mater Struct* 2: 243–255
92. Akshantala NV, Talreja R (1998) A mechanistic model for fatigue damage evolution in composite laminates. *Mech Mater* 29: 123–140
93. Silberschmidt VV (1993) Models of stochastic fracture and analysis of matrix cracking in crossply laminates under cyclic loading. Deutsche Forschungsanstalt für Luft- und Raumfahrt e.V., Braunschweig (Report DLR-IB-131-93/32)

94. McCartney LN, Schoeppner GA (2002) Predicting the effect of non-uniform ply cracking on the thermoelastic properties of cross-ply laminates. *Compos Sci Technol* 62: 1841–1856
95. McCartney LN (2005) Multiscale predictive modelling of cracking in laminate composites. In: Soutis C, Beaumont PWR (eds) *Multiscale modelling of composite material systems: the art of predictive damage modelling*. Woodhead Publishing, Cambridge, pp 65–98
96. Beaumont PWR (2003) Physical modelling of damage development in structural composite materials under stress. In: Harris B (ed) *Fatigue in composites*. Woodhead Publishing, Cambridge, pp 365–412
97. Poursartip A, Ashby MF, Beaumont PWR (1986) The fatigue damage mechanics of a carbon fibre composite laminate. I. Development of the model. *Compos Sci Technol* 25: 193–218